Microwave helicon propagation and the dynamic magnetic susceptibility in $Hg_{1-x}Mn_xSe$

D. P. Mullin,* R. R. Galazka,† and J. K. Furdyna
Department of Physics, Purdue University, West Lafayette, Indiana 47907
(Received 2 September 1980; revised manuscript received 9 February 1981)

The electronic and magnetic properties of the "semimagnetic" semiconductor $Hg_{1-x}Mn_xSe$ ($x \approx 0.06$) are studied by microwave helicon transmission. Experiments are carried out at 35 GHz in the temperature range 4.2–90 K, and in magnetic fields up to 60 kG. The helicon wave dispersion and damping provide a measurement of the free-electron concentration and mobility. Near the electron paramagnetic resonance (EPR) of the Mn^{2+} ions helicon transmission shows pronounced EPR absorption and dispersion, which yield the real and imaginary parts of the dynamic magnetic susceptibility of $Hg_{1-x}Mn_xSe$. In addition to providing the EPR position and linewidth, this measurement also determines the value of the static magnetic susceptibility of the Mn^{2+} ion subsystem.

I. INTRODUCTION

Helicon wave propagation at microwave frequencies provides a convenient, contactless method for the study of the electrical and the magnetic properties of semiconductors.[1–4] When the electrical parameters of the material satisfy the conditions for helicon wave propagation, the presence of an external magnetic field allows electromagnetic waves in the form of circularly polarized helicons to penetrate the medium to a depth considerably greater than the classical skin depth calculated using the zero-field conductivity. The sense of the propagating polarization is determined by the sign of the free carriers. When the free carriers are electrons and the solid in question contains localized paramagnetic ions, the polarization of the helicons is the same as the sense of precession of the magnetic dipoles. The helicons will then interact resonantly with the paramagnetic ions when conditions for electron paramagnetic resonance (EPR) are satisfied.

In this paper we present a study of helicon wave propagation and helicon-excited EPR in the ternary compound $Hg_{1-x}Mn_xSe$, with $x = 0.058$. This material is a narrow-gap semiconductor, with physical properties much like those of HgTe, $Hg_{1-x}Mn_xTe$, and HgSe. Because of the presence of substitutional magnetic ions in its lattice, which influence many of its electrical and optical properties, this material is sometimes referred to as a "semimagnetic" semiconductor, along with $Hg_{1-x}Fe_xTe$, $Cd_{1-x}Mn_xTe$, and others. $Hg_{1-x}Mn_xSe$ is particularly well suited for the study of helicon-excited EPR because of the simultaneous presence in the material of a high concentration of very mobile electrons and a random distribution of localized magnetic moments. The absence of holes makes the quantitative interpretation of the helicon-EPR data in a typical $Hg_{1-x}Mn_xSe$ sample particularly reliable.

In the next section, we formulate briefly the electromagnetic problem of helicon wave propagation in a conducting medium containing magnetic moments. Section III describes details of the experimental procedure, including sample preparation. The experimental results of the helicon propagation and helicon-EPR measurements, and a discussion of these results, are presented in Sec. IV.

II. ELECTROMAGNETIC PRELIMINARIES

The problem of helicon-excited EPR in a material such as $Hg_{1-x}Mn_xSe$ can be described by considering wave propagation in an isotropic plasma of highly mobile electrons in a crystalline lattice containing a random distribution of paramagnetic ions. When an external magnetic field $\vec{B} = B_0\hat{z}$ is applied, both the permittivity ϵ and the permeability μ of such a system become gyrotropic tensors, of the form

$$\vec{A} = \begin{pmatrix} A_{xx} & A_{xy} & 0 \\ -A_{xy} & A_{xx} & 0 \\ 0 & 0 & A_{zz} \end{pmatrix} . \tag{1}$$

If we assume plane-wave solutions of the form $\exp(i\vec{k}\cdot\vec{r} - i\omega t)$, we obtain from Maxwell's equations the wave equation for the electric field,[3]

$$\vec{k}\times[\vec{\eta}^{-1}\cdot(\vec{k}\times\vec{E})] + \frac{\omega^2}{c^2}\vec{\kappa}\cdot\vec{E} = 0 , \tag{2}$$

where $\vec{\eta} = \vec{\mu}/\mu_0$ is the relative permeability tensor, $\vec{k}$ is the wave vector, ω is the microwave angular fre-

quency, c is the speed of light in vacuum, $\vec{\kappa}=\vec{\epsilon}/\epsilon_0$ is the dielectric tensor, and μ_0 and ϵ_0 are the vacuum permeability and permittivity.

We shall restrict our attention to the Faraday geometry, i.e., to the case when the wave vector is parallel to $\vec{B}$. For this geometry the solutions of the wave equation are two circularly polarized modes,

$$\vec{E}_{\pm}=E_0(\hat{x}\pm i\hat{y})\exp(ik_{\pm}z-i\omega t) \ , \tag{3}$$

where the complex wave numbers $k_{\pm}$ are

$$k_{\pm}=(\omega/c)(\kappa_{\pm}\eta_{\pm})^{1/2} \ , \tag{4}$$

and

$$\kappa_{\pm}=\kappa_{xx}\pm i\kappa_{xy}, \quad \eta_{\pm}=\eta_{xx}\pm i\eta_{xy} \ . \tag{5}$$

Separating $k_{\pm}$ into real and imaginary parts,

$$k_{\pm}=\alpha_{\pm}+i\beta_{\pm} \ , \tag{6}$$

we obtain

$$\alpha_{\pm}=(\omega/\sqrt{2}c)[|\kappa_{\pm}||\eta_{\pm}|+(\kappa'_{\pm}\eta'_{\pm}-\kappa''_{\pm}\eta''_{\pm})]^{1/2} \ , \tag{7}$$

$$\beta_{\pm}=(\omega/\sqrt{2}c)[|\kappa_{\pm}||\eta_{\pm}|-(\kappa'_{\pm}\eta'_{\pm}-\kappa''_{\pm}\eta''_{\pm})]^{1/2} \ , \tag{8}$$

where the single and double primes denote real and imaginary parts of κ and η. Equations (7) and (8) determine the phase and attenuation of the wave, respectively. Using these results, we can express the signal transmitted by a sample of thickness d in terms of the complex transmission coefficient τ for an infinite plate bounded by vacuum on both sides:

$$\tau_{\pm}=(1-r_{\pm}^2)e^{ik_{\pm}d}/(1-r_{\pm}^2e^{i2k_{\pm}d}) \ . \tag{9}$$

Here $r_{\pm}$ is the reflection coefficient of a semi-infinite half space, given by

$$r_{\pm}=[1-(\kappa_{\pm}/\eta_{\pm})^{1/2}]/[1+(\kappa_{\pm}/\eta_{\pm})^{1/2}] \ . \tag{10}$$

In this paper a one-electron Drude model is used for the dielectric constant in the analysis of the electronic properties and related computer calculations. In terms of this model the dielectric constants for the two normal modes are

$$\kappa_{\pm}=\kappa_l\left[1+i\frac{\omega_p^2}{\omega}\frac{\tau}{1-i(\omega\pm\omega_c)\tau}\right] \ , \tag{11}$$

where κ_l is the lattice dielectric constant, $\omega_p\equiv(nq^2/m^*\epsilon_0\kappa_l)^{1/2}$ is the plasma frequency, n is the free-carrier concentration, q is the carrier charge, m^* is the effective mass, τ is the relaxation time, and $\omega_c=qB_0/m^*$ is the cyclotron frequency. For the material considered here, the free carriers are electrons and $q=-e$, where e is the magnitude of the electronic charge. Note that, in this convention, $\omega_c<0$ for electrons when the magnetic field B_0 is in the positive z direction.

To analyze the contribution of the localized magnetic moments, which enters the problem through $\eta_{\pm}\equiv 1+\chi_{\pm}$, where $\chi_{\pm}$ is the dynamic magnetic susceptibility, we use the Bloch model.[5] The response of the magnetic dipoles to a circularly polarized electromagnetic wave is then described by

$$\chi_{\pm}=\mp i\chi_0\omega_L T_2/[1-i(\omega\pm\omega_L)T_2] \ , \tag{12}$$

where χ_0 is the static magnetic susceptibility, T_2 is the spin-spin relaxation time, and ω_L is the Larmor precession frequency, given by $\omega_L\equiv -geB_0/2m$. Here g is the Landé g factor and m is the free electron mass. Note that the sign of ω_L is the same as of ω_c, so that the resonant response in χ is also excited by the (+) polarization, as can be seen from the denominator of Eq. (12).

For $Hg_{1-x}Mn_xSe$ crystals of good quality the sample parameters appearing in $\kappa_{\pm}$ typically satisfy the relations

$$|\omega_c\tau|>>1, \quad |\omega_c|>>\omega, \quad \omega_p^2>>|\omega\omega_c| \ , \tag{13}$$

for microwave frequencies and for magnetic fields exceeding a few kilogauss. The third inequality indicates that under typical experimental conditions the lattice dielectric constant is a negligible part of $\kappa'_{\pm}$. The parameter ranges where inequalities (13) are satisfied constitute the "helicon limit."[2,4] Within this limit the effective dielectric constants assume simple approximate forms, and in turn the propagation coefficients $\alpha_{\pm}$ and $\beta_{\pm}$ in Eqs. (7) and (8) can be simplified to

$$a_+\approx(ne\omega\mu_0/B_0)^{1/2}(1+\tfrac{1}{2}\chi'_+) \ , \tag{14}$$

$$\beta_+\approx\frac{1}{2}\left(\frac{ne\omega\mu_0}{B_0}\right)^{1/2}\left(\frac{1}{|\omega_c|\tau}+\chi''_+\right)<<\alpha_+ \ , \tag{15}$$

$$\alpha_-\approx\frac{1}{2}\left(\frac{ne\omega\mu_0}{B_0}\right)^{1/2}\left(\frac{1}{|\omega_c|\tau}+\chi''_-\right)<<\alpha_+ \ , \tag{16}$$

$$\beta_-\approx(ne\omega\mu_0/B_0)^{1/2}(1+\tfrac{1}{2}\chi'_-)>>\beta_+ \ , \tag{17}$$

where we have not made any simplifications for χ except to assume that $|\chi|<<1$, as is appropriate for a paramagnetic system. It will be seen that the contribution of χ to α and β will be negligible except in the immediate vicinity of EPR. From these expressions it is evident that the (+) polarization propagates with relatively low damping and comprises the helicon waves referred to previously. The (−) polarization is characterized by strong attenuation and nearly total reflection. Because of this, and of the fact that EPR occurs in the (+) polarization, the remainder of this discussion will deal only with the (+) polarization.

From Eq. (14) we see that the helicon dispersion is a sensitive function of n and can be used to determine this parameter. The carrier mobility μ_e can be subsequently determined from the magnetic field dependence of the attenuation, Eq. (15), which depends on $|\omega_c|\tau=\mu_eB_0$. With n and μ_e determined

(from data away from EPR, where the contribution of χ is negligible), measurements of helicon dispersion and absorption in the EPR vicinity can then be used to obtain the value of the dynamic susceptibility χ_+.

III. EXPERIMENT

The microwave transmission experiments were performed in the Faraday geometry using a 35-GHz Rayleigh interferometer bridge.[6] Such an interferometer allows the measurement of the amplitude and phase of the signal transmitted by the sample. The bridge, shown schematically in Fig. 1, consists of a sample arm and a reference (bypass) arm. Most of the microwave power enters the sample arm and is converted to circular polarization before it is incident on the sample; and a small fraction of the power can be routed through the reference arm, bypassing the sample. This provides a means of measuring the magnetic field dependence of the phase of the signal transmitted through the sample when it is recombined and interfered with the reference arm signal. A ferrite modulator operated at 1000 Hz is used to amplitude-modulate the sample arm signal only. The use of lock-in detection rejects that part of the signal at the detector which is due solely to the reference arm transmission. The detected signal is plotted on an

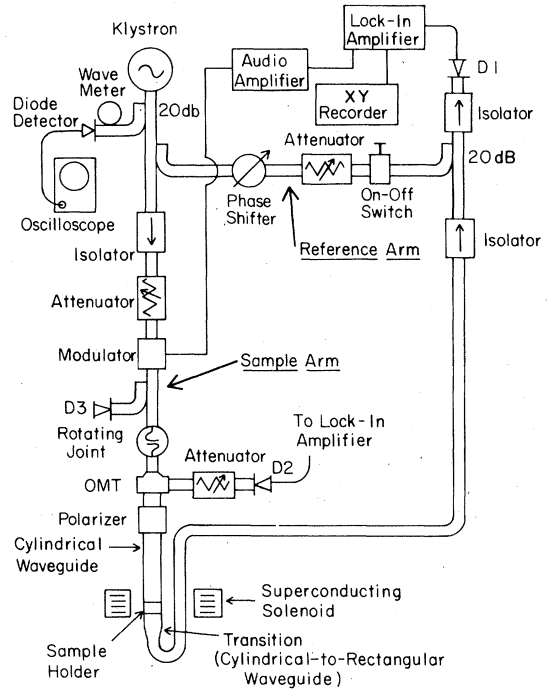

FIG. 1. Schematic diagram of the 35-GHz microwave spectrometer.

XY recorder, and is given by[3]

$$\langle P\rangle = C[|\tau_+|^2 + 2|\tau_+|A_R\cos(\Theta_\tau - \Theta_R)] \ , \quad (18)$$

where C is a proportionality constant involving the amplifier gain, recorder scale factors, bridge attenuator settings, etc. Here the amplitude of the signal routed through the reference arm is A_R, and Θ_τ and Θ_R are the phases of the sample and reference signals, respectively. The value of Θ_τ depends on magnetic field through $\alpha_+ d$.

The sample of $Hg_{1-x}Mn_xSe$ was cut in the shape of a thin disk of thickness $d = 0.399$ mm and was mounted so as to completely block the waveguide. A highly conducting silver paste effectively sealed the sample to the waveguide, preventing leakage of microwave power around the sample.

The magnetic field was produced by a 6-T superconducting solenoid. An insert Dewar enclosing the sample holder permitted measurements at temperatures from 4.2 to 90 K. The temperature was measured with a GaAs light-emitting diode (LED)[7] mounted on the sample holder in the immediate proximity of the sample. This LED was calibrated with a Chromel-(Au + 0.07 at.%Fe) thermocouple.

The sample of $Hg_{1-x}Mn_xSe$ was grown from the melt by a modified Bridgman method at the Institute of Physics, Polish Academy of Sciences. According to known phase diagrams,[8] this material crystallizes in the zinc-blende crystallographic structure (the same as HgSe) up to $x \approx 0.35$. The crystals are n type as a result of a natural tendency of this material to deviate slightly from stoichiometry in the process of crystal formation. A typical electron concentration in as-grown HgSe and $Hg_{1-x}Mn_xSe$ samples is ca. $n \approx 5 \times 10^{24}$ m^{-3}. To reduce the number of donors, the sample used in this investigation was annealed for 98 h in Se vapor at 180 °C, followed by 235 h in static vacuum at 120 °C. The composition of the sample was determined by density measurements to have a Mn content of $x = 0.058 \pm 0.002$.

IV. RESULTS AND DISCUSSION

A. Helicon wave propagation and electrical parameters

Direct transmission data (i.e., the signal observed when the reference arm signal is zero) for the $Hg_{1-x}Mn_xSe$ sample at 10 K is shown in Fig. 2(a). The transmission maxima seen here are Fabry-Perot dimensional resonances. Their presence indicates good sample homogeneity and a respectable electron mobility. Figure 2(b) shows a calculation of the direct transmission using the parameters obtained from the analysis of the dispersion and damping exhibited by this sample at low fields (see Fig. 3), $n = 2.70 \times 10^{23}$ m^{-3} and $\mu_e = 8.40$ m^2/V sec. We ob-

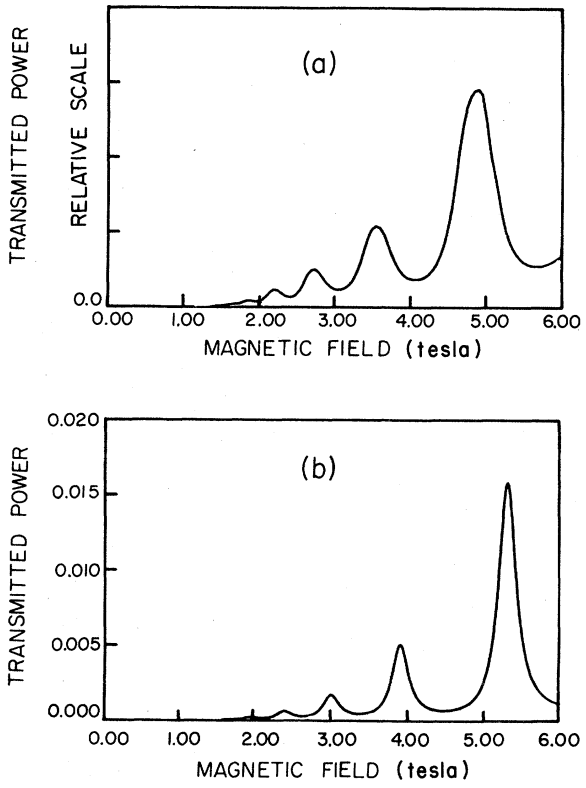

FIG. 2. Transmitted microwave power as a function of magnetic field: (a) data for $Hg_{1-x}Mn_xSe$ sample, $x=0.058$, observed at $T=10$ K; (b) calculation for $n=2.7\times10^{23}$ m^{-3}, $\mu_e=8.4$ m^2/V sec.

serve a good qualitative agreement between the two graphs, except for a shift in the positions of the Fabry-Perot maxima and for the half-widths of the resonances. This last discrepancy could be due to the faces of the sample being slightly nonparallel, to inhomogeneity in the electron concentration across the sample, or to a gradual decrease of the electron mobility with magnetic field. The shift in the position of the resonances is a problem that is not unique to this sample: we have observed such shifts in other specimens (e.g., InSb) in the course of our investigation of helicon waves. It is not due to an error in the carrier concentration, because the periodicity in $B_0^{-1/2}$ of the resonances is the same for both graphs, and agrees very well with the electron concentration obtained from the low-field phase-shift data. A plausible explanation for this shift is the presence of an unwanted reflection within the sample holder, probably between the sample and the waveguide U bend. Such a reflection could significantly alter the impedance at the sample-waveguide interface, introducing a constant phase shift in the signal reflected at the interface, and thus making the resonance condition different from that obtained when the sample is bounded by free space on both sides. Using computer calculations, we have demonstrated that when the original slab sample is replaced by a sandwich of the sample and a lossless dielectric, the actual positions of the dimensional resonances are shifted, but the periodicity in $B_0^{-1/2}$ is not altered.

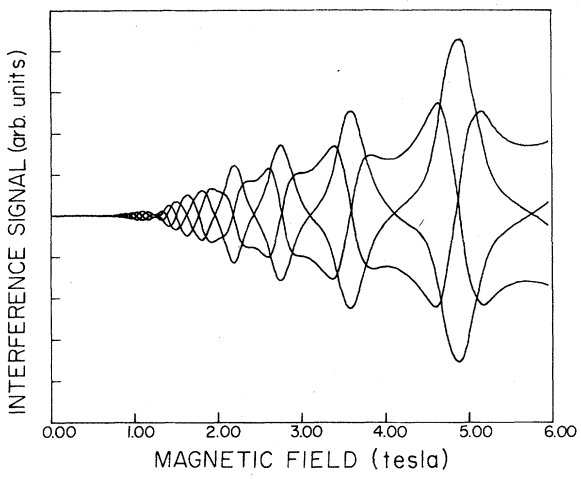

FIG. 3. Interference traces for the (+) polarization obtained at four phase settings of the reference arm, 90° apart, at $T=10$ K.

Figure 3 shows a Rayleigh interferogram for this sample at a temperature of 10 K and for magnetic fields up to 6.0 T. The four traces correspond to four settings of the phase shifter that are 90° apart. The amplitude maxima seen here correspond to the Fabry-Perot maxima seen in Fig. 2. Note that the data display not only these well-known oscillations in the amplitude of the transmitted signal, but also oscillations in the *phase* of the transmitted wave about the monotonic $B_0^{-1/2}$ magnetic field dependence which the phase would have in the absence of multiple internal reflections. This effect is shown in Fig. 4, where the oscillatory curve is the observed phase change as a function of magnetic field, taken from Fig. 3 at fields above 3.5 T. The straight line in Fig. 4 is an extrapolation of the rate of phase change from low magnetic fields, where no oscillations in amplitude or phase are observed. Although such phase oscillations are clearly present in the expression for the complex transmission coefficient τ, Eq. (9), we are not aware of any experimental observations of this *dispersive* aspect of the Fabry-Perot effect elsewhere in the literature.

The low-field Rayleigh interferograms obtained on this sample of $Hg_{1-x}Mn_xSe$ were computer-fitted in the region well away from the magnetic resonance, to establish the electron concentration and mobility. This region is illustrated by Fig. 5 below, say, 1.10 T.

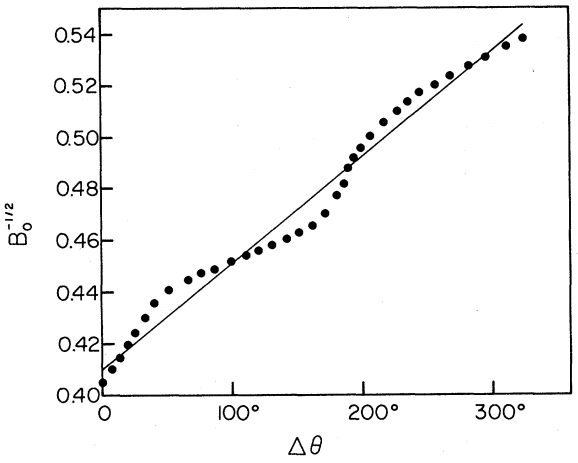

FIG. 4. Relative phase change of the transmitted signal plotted as a function of $B_0^{-1/2}$. The circles are data points taken from the high-field region of Fig. 3. The straight line is an extrapolation of the rate of phase change observed at low fields.

This figure shows two sets of data (solid circles) obtained at 10 K for two phase settings of the reference arm, 90° apart; and two calculated interference traces, obtained using Eq. (18) for two values of θ_R 90° out of phase (solid lines). The best-fit parameters used in this calculation were $n = 2.7 \times 10^{23}$ m^{-3} and $\mu_e = 8.4$ m^2/V sec. The agreement of the data with the calculation is quite good here and is typical of the fits obtained at other temperatures. The electron concentration was found to be constant at $n = 2.7 \times 10^{23}$ m^{-3} from 90 to 4.2 K, while the mobility increased from 5.6 m^2/V sec at 90 K to 8.65 m^2/V sec at 4.2 K.

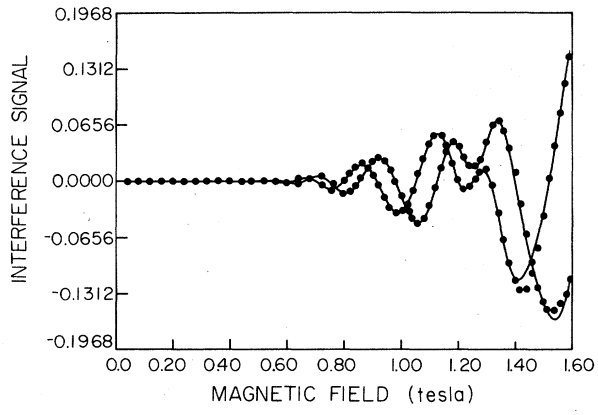

FIG. 5. Theoretical fits for two helicon interference traces differing in phase by 90°. The circles are data points (taken at 10 K), and the solid lines are calculated for $n = 2.7 \times 10^{23}$ m^{-3}, $\mu_e = 8.4$ m^2/V sec.

B. Dynamic magnetic susceptibility

Having determined the electronic properties by using data away from EPR (e.g., $B < 1.1$ T in Fig. 5), we were then able to computer-fit the absorption and dispersion in the neighborhood of the magnetic resonance (e.g., $1.1 \lesssim B \lesssim 1.4$ T in Fig. 5). A Bloch model for the magnetic susceptibility χ_+ of a two-level spin system was used for fitting the real and imaginary parts of the dynamic magnetic susceptibility χ_+ in these calculations. The Mn^{++} system is, of course, in reality much more complicated than a two-level system described by the Bloch model, but because of the extreme width of the resonance the use of a more detailed model, including fine and hyperfine interactions, does not affect the width of the resonance and causes only a very small change in its strength. The amplitude of the dynamic susceptibility provides, in turn, the value of the static magnetic susceptibility χ_0 [see Eq. (12)]. The spin-spin relaxation time T_2 is used here only as a fitting parameter to simulate the width of the resonance. The position of the resonance provides a value for the g factor. However, because the resonance line is very broad, we have not attempted to determine the value of g with accuracy. Rather, we have used a value of $g = 2.00$, which was obtained for Mn^{++} in other II–VI compounds.[9,10]

As can be seen from Eqs. (14) and (15), the helicon method of exciting EPR provides a direct measurement of the values of the real and imaginary parts of the dynamic magnetic susceptibility χ_+. These two quantities are shown as functions of magnetic field for several temperatures in Figs. 6 and 7. The susceptibility is expressed in dimensionless units, consistent with the mks definition in Eq. (12). We observe that as the temperature decreases, the strength of the resonance increases, as would be expected from the usual temperature dependence of χ_0. However, the width of the line also increases dramatically. This suggests the presence of a strong spin-spin interaction which leads to the broadening of the resonance line at low temperatures. It is also seen that the dispersive effects of the magnetic ions are quite strong at a distance of several kilogauss from the resonance at low temperatures, while the effect of absorption is less extended, as is the nature of Lorentzian lines.

C. Static magnetization

The process of fitting Eq. (12) to the magnetic resonance absorption and dispersion yields a value of the parameter χ_0, which, within the framework of the Bloch model, is identified as the static magnetic susceptibility. In more complicated situations involving, e.g., significant antiferromagnetic interaction, such as

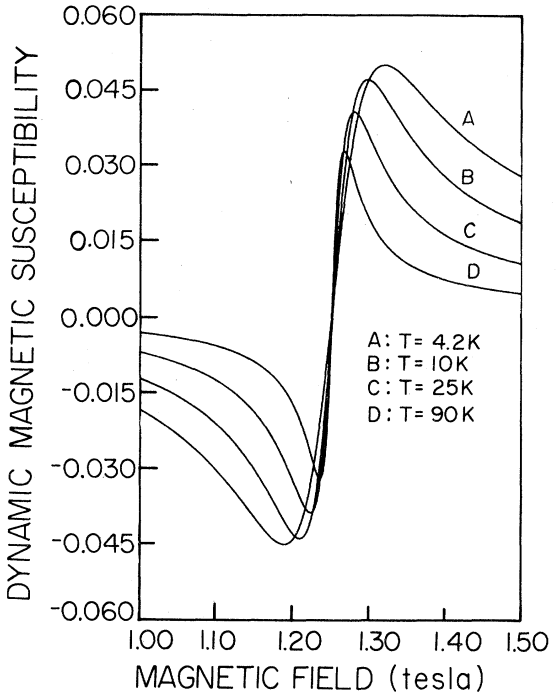

FIG. 6. Real part of the dynamic magnetic susceptibility as a function of magnetic field at four temperatures. The susceptibility is obtained by fitting data such as in Fig. 5.

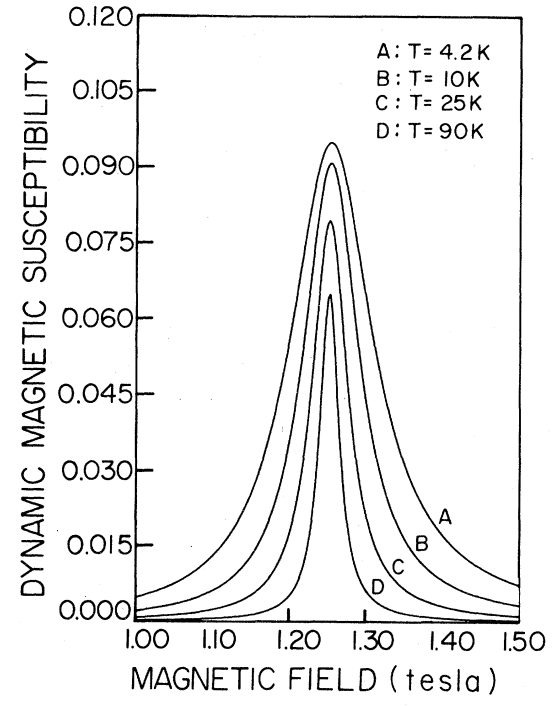

FIG. 7. Imaginary part of the dynamic magnetic susceptibility as a function of magnetic field, obtained at four temperatures from data such as in Fig. 5.

should be in effect in the present case, this quantity may differ significantly from the low-field dc susceptibility, since our χ_0 is determined at relatively high fields. It should therefore be understood as a measure of magnetization ($\chi_0 = M/H$) at those fields.

In earlier studies[3] the helicon method has given reasonable values of χ_0, exhibiting normal paramagnetic behavior in samples of $Hg_{1-x}Mn_xTe$ for low values of x. The values of the parameter χ_0 determined by the fitting procedure for the present sample are plotted in Fig. 8 as $1/\chi_0$ versus temperature. At higher temperatures the behavior is approximately Curie-Weiss-like, with a Curie temperature of $\Theta \approx -36$ K obtained from the extrapolation of the high-temperature data points to $1/\chi_0$ equal to zero. It is readily seen, however, that at low temperatures the susceptibility deviates from a Curie or Curie-Weiss behavior. A similar deviation from Curie-Weiss behavior has been observed in the case of dc susceptibility measurements in $Hg_{1-x}Mn_xTe$, $Hg_{1-x}Mn_xSe$, and $Hg_{1-x}Mn_xS$.[11-13]

One of the interesting properties of such semiconducting compounds containing substitutional magnetic ions ("semimagnetic" semiconductors) which has led to a great deal of recent work is the effect of the magnetization on the behavior of the energy-band parameters, especially in the presence of an external magnetic field. Optical and electrical properties of such ternary alloys are particularly sensitive to the magnetization of this built-in system of spins. In the interpretation of the Shubnikov–de Haas measurements on $Hg_{1-x}Mn_xTe$,[14] $Hg_{1-x}Mn_xSe$,[15] and of magneto-optical[16] measurements on $Hg_{1-x}Mn_xTe$, it has been necessary to use a magnetization that is less than that due to isolated ions to fit the data at liquid-helium temperatures. This inference of a reduced low-temperature magnetization is consistent

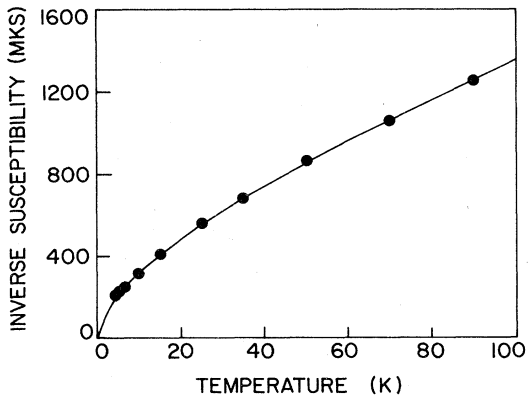

FIG. 8. Inverse dc magnetic susceptibility χ_0 as a function of temperature. The dots represent experimental data. The continuous line is a guide for the eyes.

with our observation of a smaller value of χ_0 than would be given by isolated magnetic ions.

Deviations from a linear dependence of $1/\chi_0$ on temperature were also observed in recent low-field dc magnetic susceptibility studies of $Hg_{1-x}Mn_xTe$ (Ref. 17) and $Cd_{1-x}Mn_xTe$ (Ref. 18) for a wide range of x values. A cluster model with a nonstatistical distribution of cluster sizes was invoked in Refs. 17 and 18 to explain the observed specific heat and magnetic susceptibility data. A transition from a paramagnetic to a spin-glass phase was observed in both materials for large values of x ($x > 0.17$).

We will not attempt a quantitative analysis of our data in terms of such a model because the exact relationship between the dc magnetic susceptibility and our quantity χ_0 is uncertain, especially since this quantity is extracted from a high magnetic field ($B \approx 1.25$ T) measurement. The high-field behavior can only be expected to increase the complexity of a magnetic system that is not yet fully understood. However, we do want to draw attention to the helicon method of examining the magnetic properties of suitable materials. The qualitative comparison of our results with dc measurements suggests that this method may prove very useful in a fuller understanding of the behavior of these materials.

D. EPR linewidth

The final aspect of the helicon-EPR studies of $Hg_{1-x}Mn_xSe$ to be considered is the increase in resonance linewidth with decreasing temperature. Figure 9 shows a plot of the full width at half-maximum of the resonance line as a function of temperature. It can be seen that there is over a fourfold increase in linewidth as the temperature is reduced from 90 to 4.2 K.

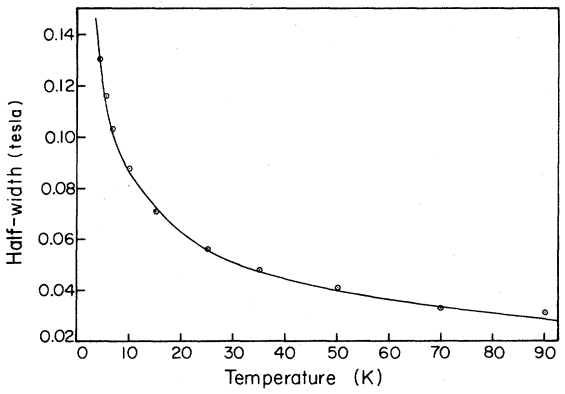

FIG. 9. Half-width of the observed EPR resonance as a function of temperature.

Such behavior has been observed in concentrated magnetic systems, such as MnTe,[19] MnSe,[20] and MnS (Ref. 21) and is interpreted in these materials as due to a transition from a paramagnetic to an antiferromagnetic state. The dependence of linewidth on temperature can in these instances be described by the relation[20]

$$\Delta H = A\left(\frac{T_c}{T - T_c}\right)^P + B \ , \tag{19}$$

where A and B are constants, T_c is the critical temperature, and P is the critical-temperature exponent.

The EPR spectra of semimagnetic semiconductors also show this behavior for a large concentration of magnetic ions.[22–24] This aspect has been, so far, investigated in $Cd_{1-x}Mn_xTe$ and $Hg_{1-x}Mn_xTe$ at values of $x > 0.20$. For such high values of x a critical temperature $T = T_c$ is observed, below which the magnetic resonance does not occur. This critical temperature is found to increase with x. For $x < 0.20$, $T_c \rightarrow 0$ K, so that the resonance, although increasing in width with decreasing temperature, is observed at all temperatures. The disappearance of the resonance has been attributed by the investigators to an order-disorder transition from the paramagnetic to the antiferromagnetic phase. It is interesting to note in this connection that recent results for $Hg_{1-x}Mn_xTe$ (Ref. 17) and $Cd_{1-x}Mn_xTe$ (Ref. 18) indicate a paramagnetic-to-*spin-glass* transition occurring near $x = 0.17$ for $T = 0$ K, with the transition temperature increasing for higher x. On the basis of this we suggest, therefore, that it is the transition to the *spin-glass* phase which is responsible for the disappearance of the resonance. Where the resonance is observed, the linewidth data can be fitted well with Eq. (19), which, however, must be viewed as empirical. There is not yet available a theory for EPR effects in such mixed systems that permits the interpretation of these results.

In the present case of $Hg_{1-x}Mn_xSe$ the observed change in linewidth with temperature is considerably larger than reported for other semimagnetic semiconductors with a comparable composition. However, if we replace $T_c/(T - T_c)$ by $1/T$ in Eq. (19) (since no transition occurs for this value of x), we obtain a value of $P = 0.47$, in good agreement with values of 0.40 to 0.47 previously obtained by other workers for semimagnetic semiconductors with larger values of x. The parameter A is found to have a value of 0.26 T, considerably larger than the values obtained by previous workers, reflecting the fact that we observe a much larger change in linewidth for a (comparatively) small value of x.

Unlike previous magnetic susceptibility and EPR linewidth measurements, we have simultaneously measured both quantities, and we believe that they

must be explained together. The usefulness of such data in explaining exchange phenomena remains to be determined. Existing theories which deal with the magnetization of these materials are still highly qualitative, and the connection with the linewidth remains to be made.

ACKNOWLEDGMENTS

We wish to thank the National Science Foundation for the support of this research through the NSF-MRL Grant No. DMR77-23798.

---

*Present address: Naval Ocean Systems Center, San Diego, Calif. 92152.

†On leave from the Institute of Physics, Polish Academy of Sciences, 02-668 Warszawa, Poland.

[1]J. D. Wiley, P. S. Peercy, and R. N. Dexter, Phys. Rev. 181, 1173 (1969).

[2]E. D. Palik and J. K. Furdyna, Rep. Prog. Phys. 33, 1193 (1970).

[3]R. T. Holm and J. K. Furdyna, Solid State Commun. 15, 1459 (1974); Phys. Rev. B 15, 844 (1977).

[4]R. S. Brazis, J. K. Požela, and J. K. Furdyna, Phys. Status Solidi A 53, 11 (1979); 54, 11 (1979).

[5]F. Bloch, Phys. Rev. 70, 460 (1946).

[6]J. K. Furdyna, Rev. Sci. Instrum. 37, 462 (1966).

[7]B. F. Griffing and S. A. Shivashankar, Rev. Sci. Instrum. 48, 1225 (1977).

[8]A. Pajaczkowska and A. Rabenau, Mater. Res. Bull. 12, 183 (1977).

[9]K. Leibler, in *International Conference on Magnetic Resonance and Relaxation, Ljubljana, 1966,* edited by R. Blinc (North-Holland, Amsterdam, 1967), p. 373.

[10]K. Leibler, W. Giriat, K. Checinski, and Z. Wilamowski, in *International Conference on Magnetic Resonance and Related Phenomena, Bucharest, 1970,* edited by I. Ursu (Institute of Atomic Physics, Bucharest, 1971), p. 987.

[11]H. Savage, J. J. Rhyne, R. Holm, J. R. Cullen, C. E. Carroll, and E. Wohlfarth, Phys. Status Solidi B 58, 685 (1973).

[12]U. Sondermann and E. Vogt, Physica (Utrecht) 86–88B, 419 (1977).

[13]A. Pajaczkowska and R. Pauthenet, J. Magn. Magn. Mater. 10, 84 (1979).

[14]M. Jaczynski, J. Kossut, and R. R. Galazka, Phys. Status Solidi B 88, 73 (1978).

[15]S. Takeyama and R. R. Galazka, Phys. Status Solidi B 96, 413 (1979).

[16]G. Bastard, C. Rigaux, Y. Guldner, J. Mycielski, and A. Mycielski, J. Phys. (Paris) 39, 87 (1978).

[17]S. Nagata, R. R. Galazka, G. D. Khattak, D. Mullin, H. Akbarzadeh, J. K. Furdyna, and P. H. Keesom, Phys. Rev. B 22, 3331 (1980).

[18]R. R. Galazka, S. Nagata, and P. H. Keesom, Phys. Rev. B 22, 3344 (1980).

[19]K. Leibler, K. Checinski, R. R. Galazka, W. Giriat, and H. Szymczak, Phys. Status Solidi B 47, K127 (1971).

[20]T. Grochulski, M. Gutowski, A. Pajaczkowska, and W. Zbieranowski, Phys. Status Solidi A 47, K169 (1978).

[21]J. W. Battles, J. Appl. Phys. 42, 1286 (1971).

[22]K. Leibler, A. Sienkiewicz, K. Checinski, R. Galazka, and A. Pajaczkowska, in *Proceedings of the III International Conference on the Physics of Narrow Gap Semiconductors, Warsaw, 1977,* edited by J. Rauluszkiewicz, M. Górska, and E. Kaczmarek (Polish Scientific Publishers, Warsaw, 1977), p. 199.

[23]K. Leibler, Z. Wilamowski, and A. Sienkiewicz, in *Proceedings of the International Symposium on Microwave Diagnostics of Semiconductors, Porvoo, Finland, 1976,* edited by R. Paananen (Swedish Academy of Engineering Sciences in Finland, Finland, 1977), p. 75.

[24]S. Oseroff, R. Calvo, and W. Giriat, J. Appl. Phys. 50, 7738 (1979).